

Formation of complex molecules after cosmic ion bombardment and UV photolysis of interstellar ice analogues

Maria Elisabetta Palumbo

INAF – Osservatorio Astrofisico di Catania

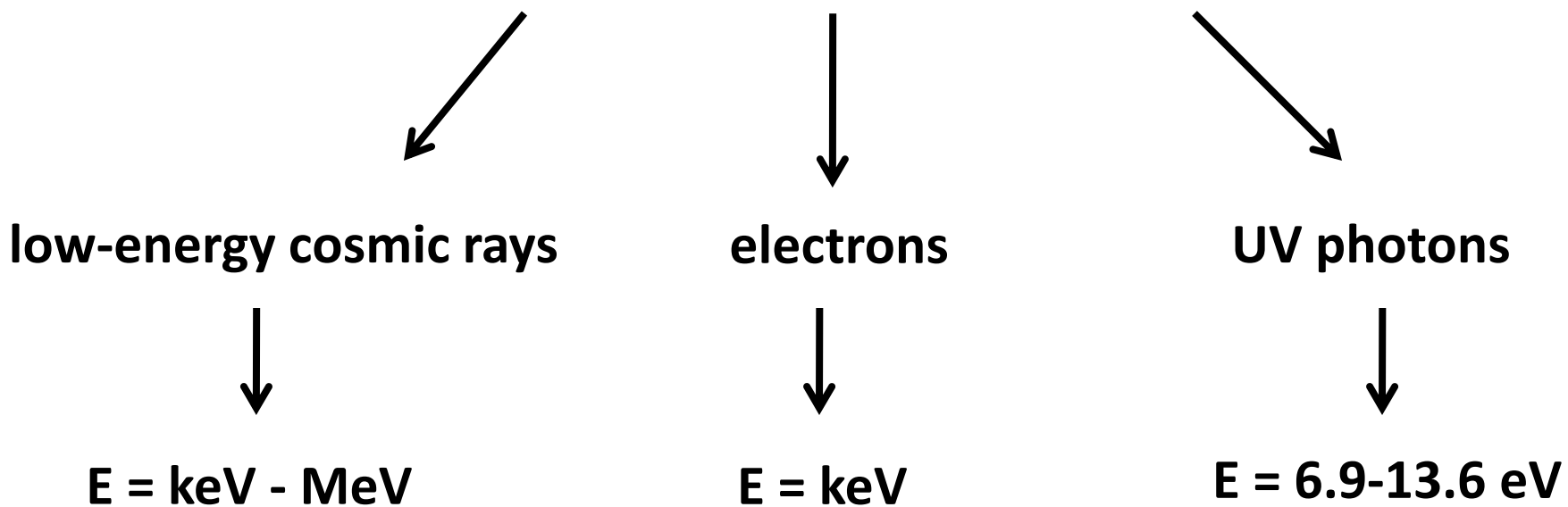
mepalumbo@oact.inaf.it

<http://www.oact.inaf.it/weboac/labsp/index.html>

Energetic processing in dense molecular clouds

High density and high extinction → stellar radiation does not penetrate molecular clouds

Interaction of cosmic rays with molecular clouds

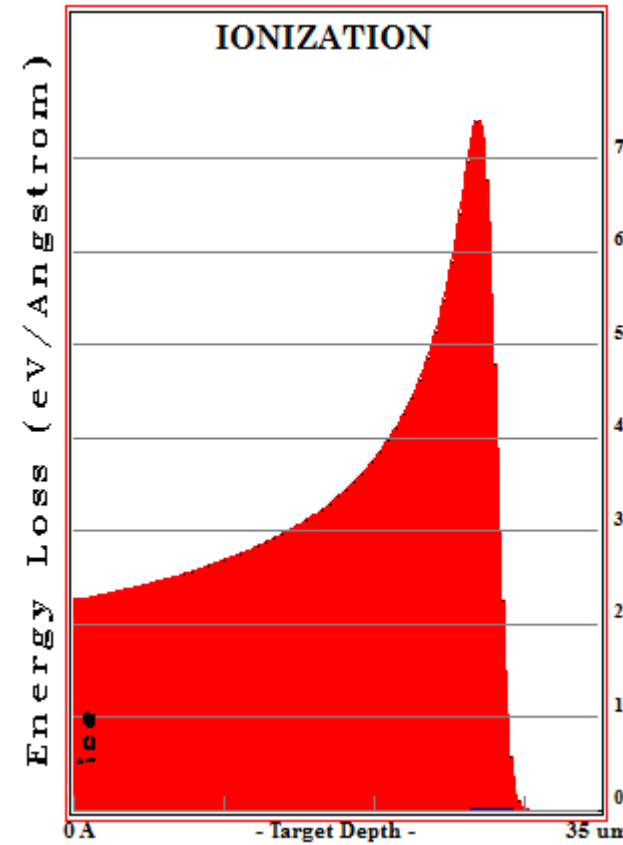
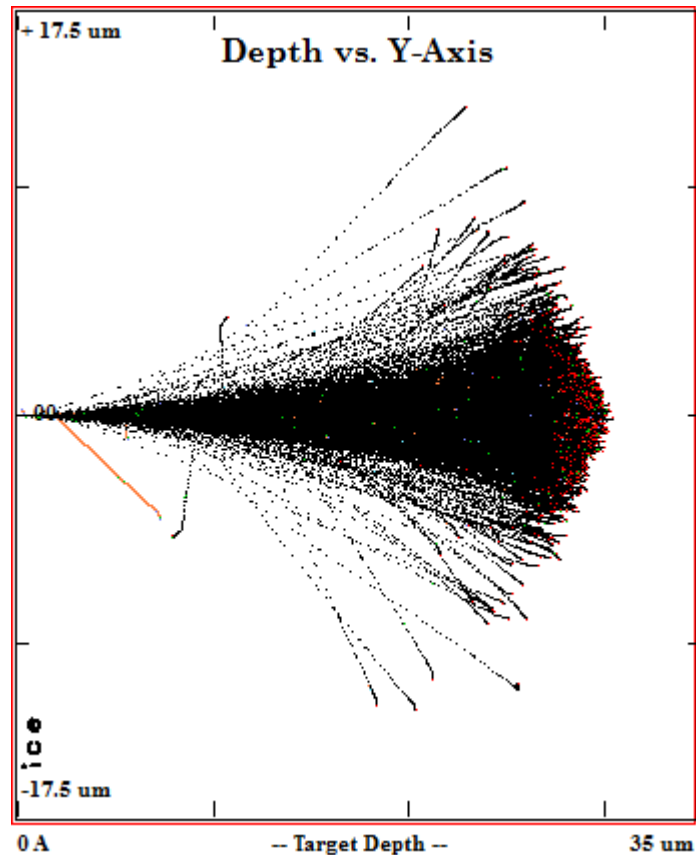


Energetic processing in the Solar System

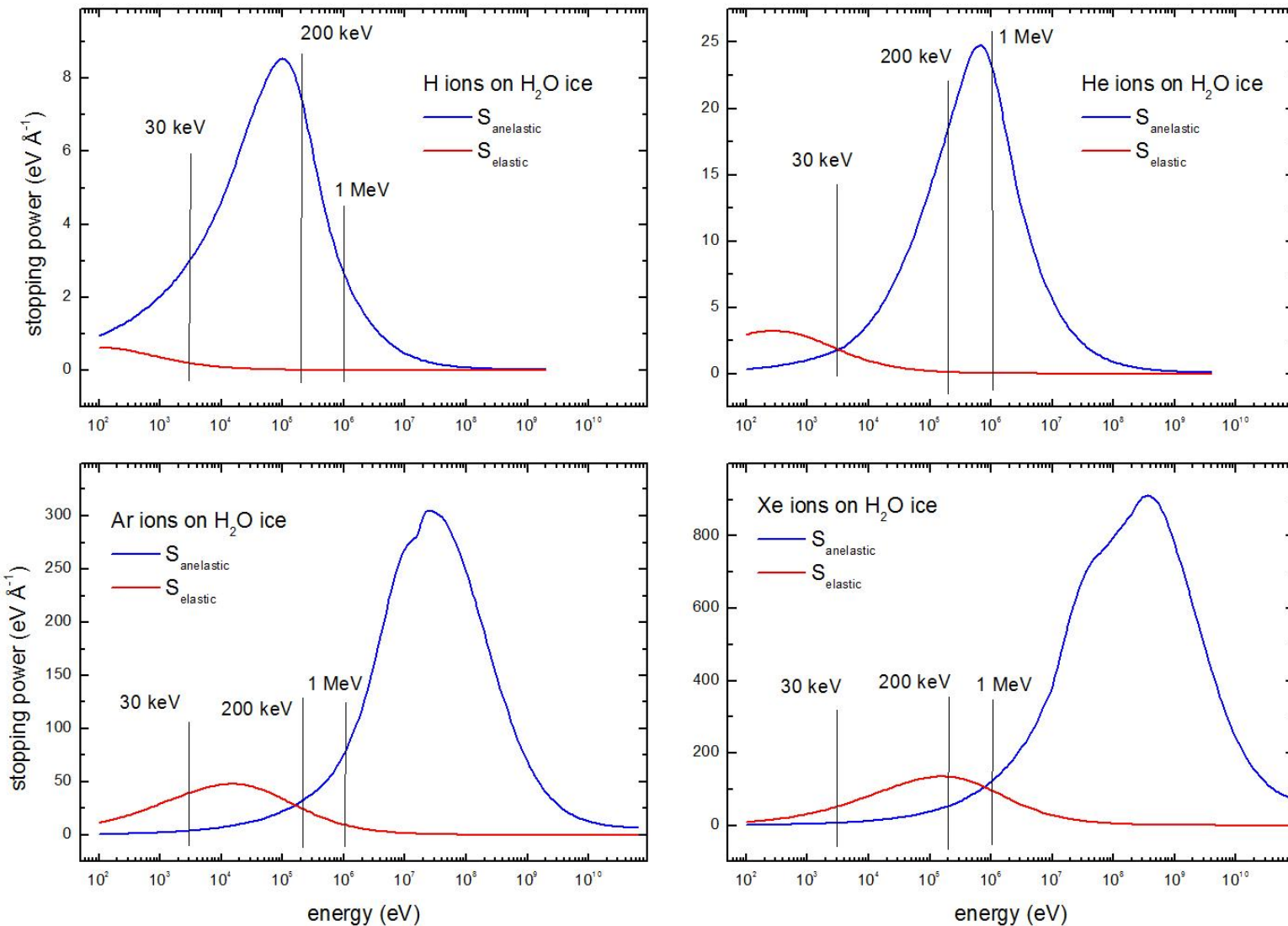
	Energy		Fluxes ($\text{cm}^{-2} \text{ s}^{-1}$)
Solar Photons	2 eV	Visible	$2.0 \cdot 10^{17}$
	4 eV	NUV	$1.5 \cdot 10^{16}$
	6 eV	FUV	$3.0 \cdot 10^{13}$
Solar Wind (1 AU)	1keV	H ⁺	$3.0 \cdot 10^8$
	4keV	He ²⁺	
Solar Flares (1 AU)	>1 MeV	H ⁺	$10^{10} (\text{cm}^{-2} \text{ yr}^{-1})$
	>1 MeV	He ²⁺	
Galactic cosmic rays	>1 MeV	H ⁺	1-10
	>1 MeV	He ²⁺	

Interaction of ions with matter

1 MeV protons on H₂O

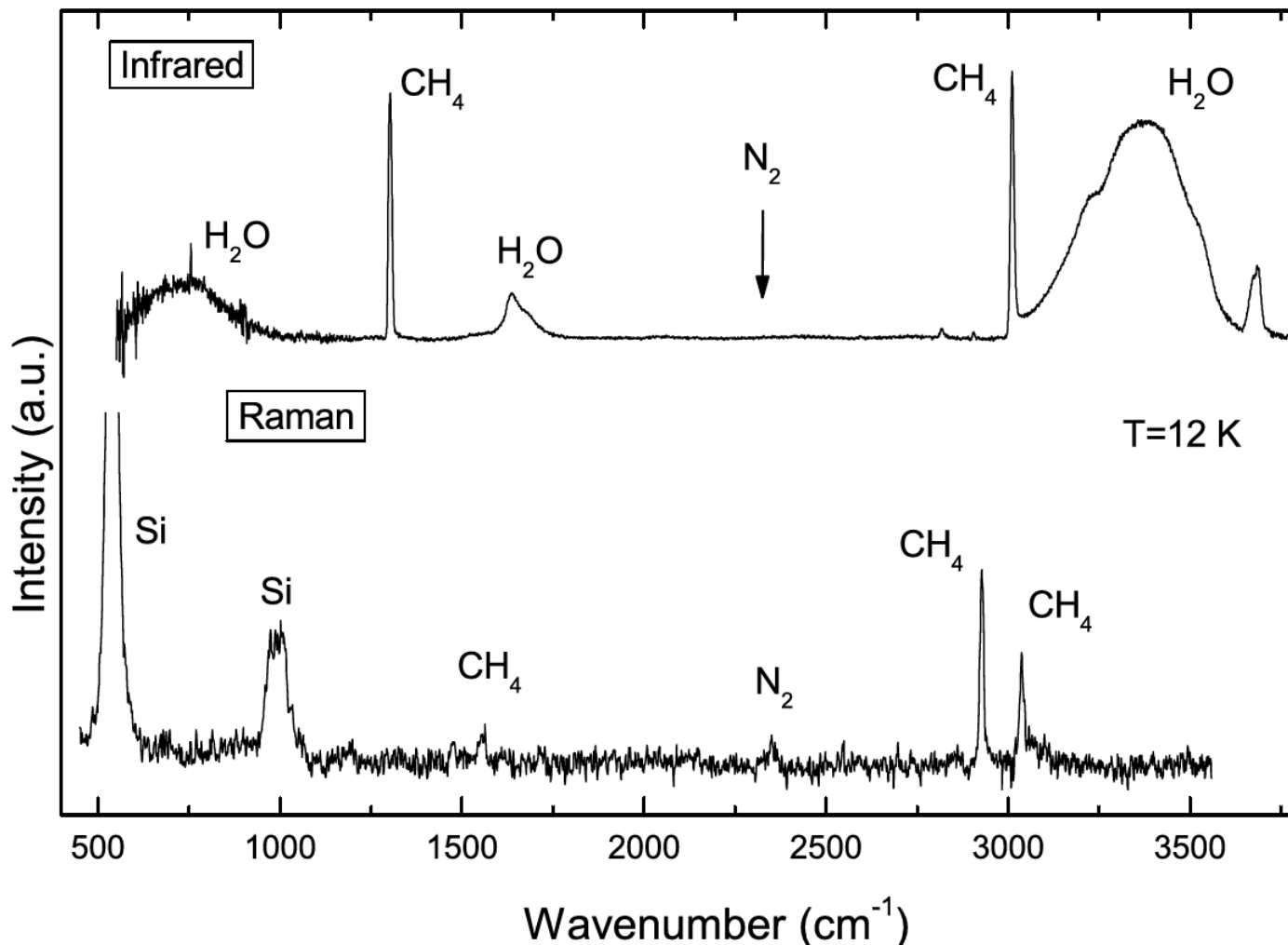


Interaction of ions with matter

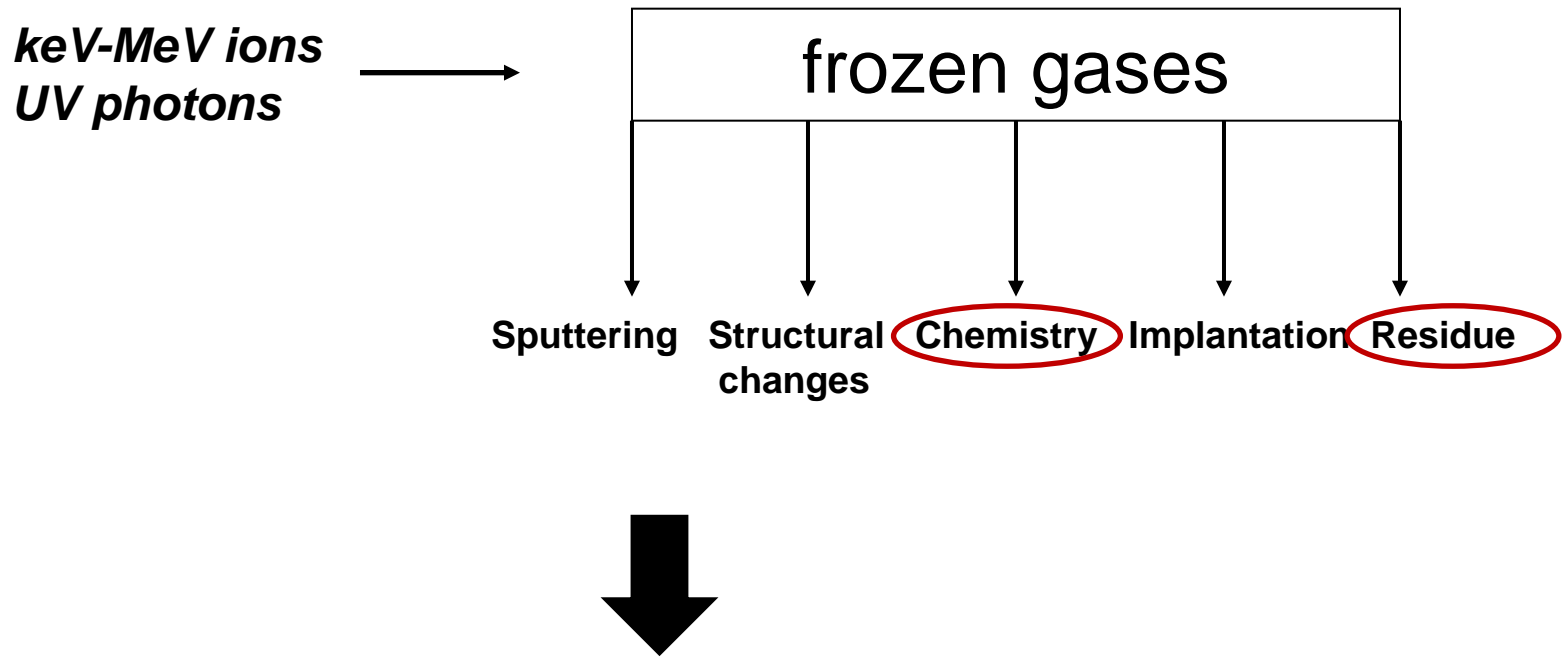


IR and Raman spectroscopy

$\text{H}_2\text{O}:\text{CH}_4:\text{N}_2$ (1:1:1)

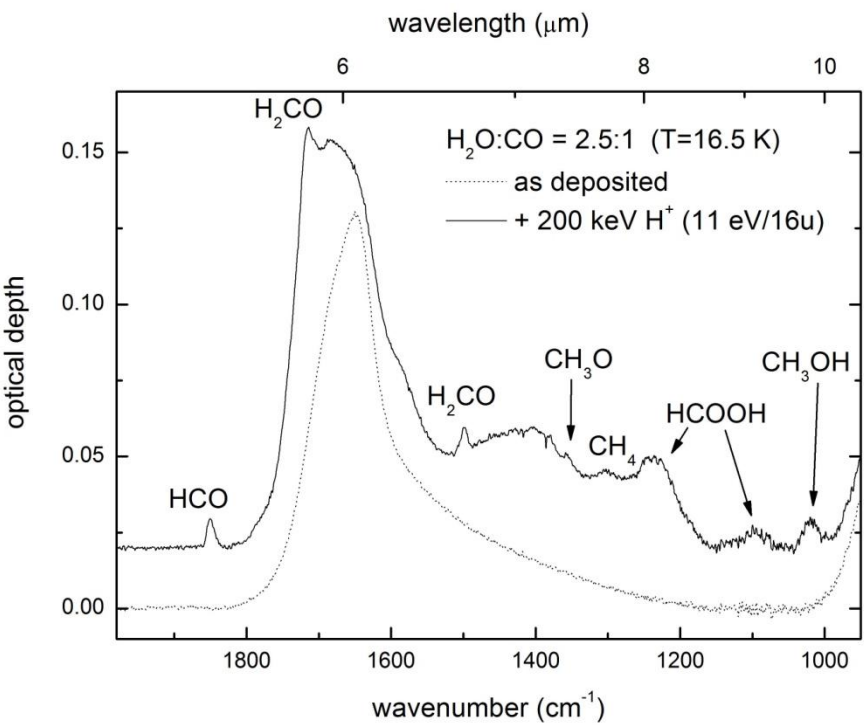
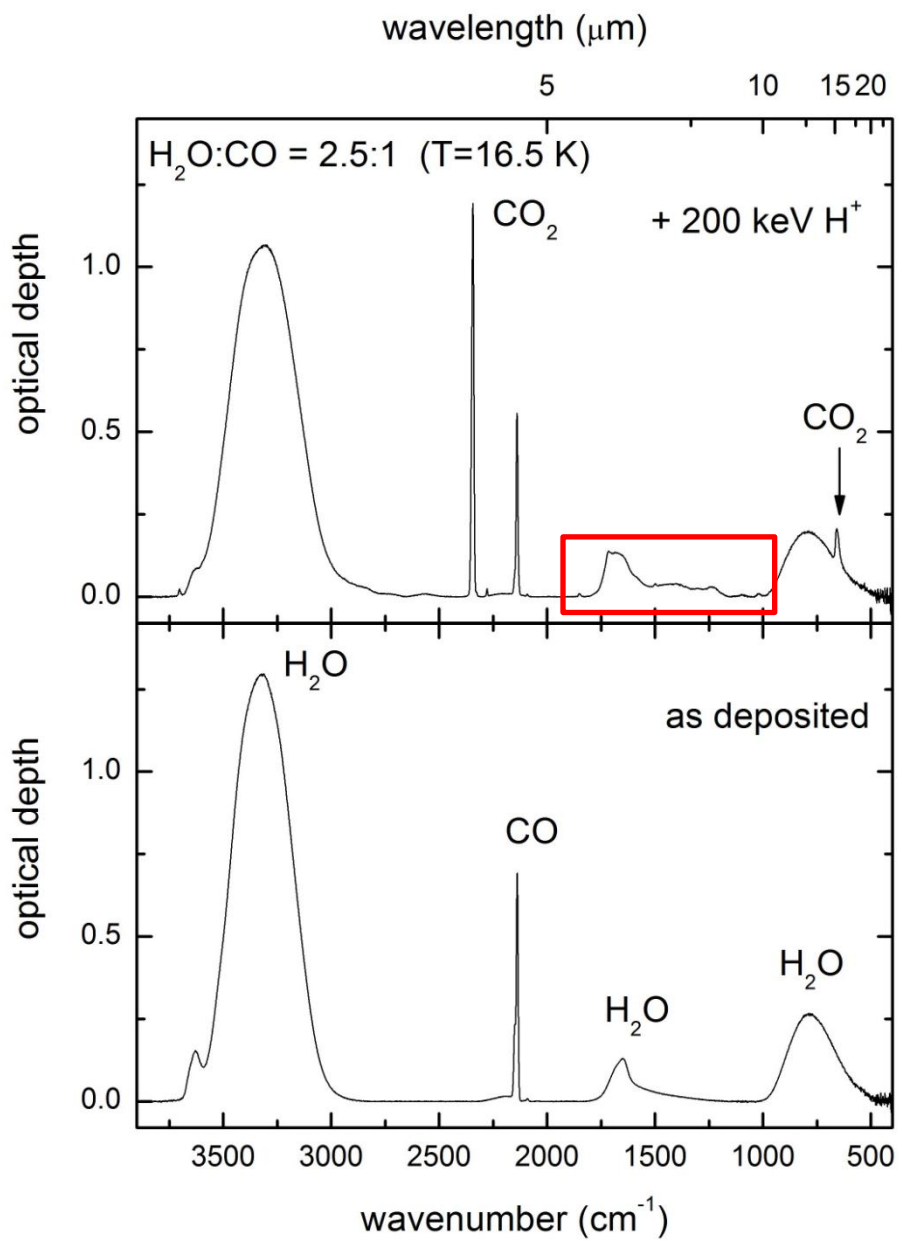


Effects of energetic processing

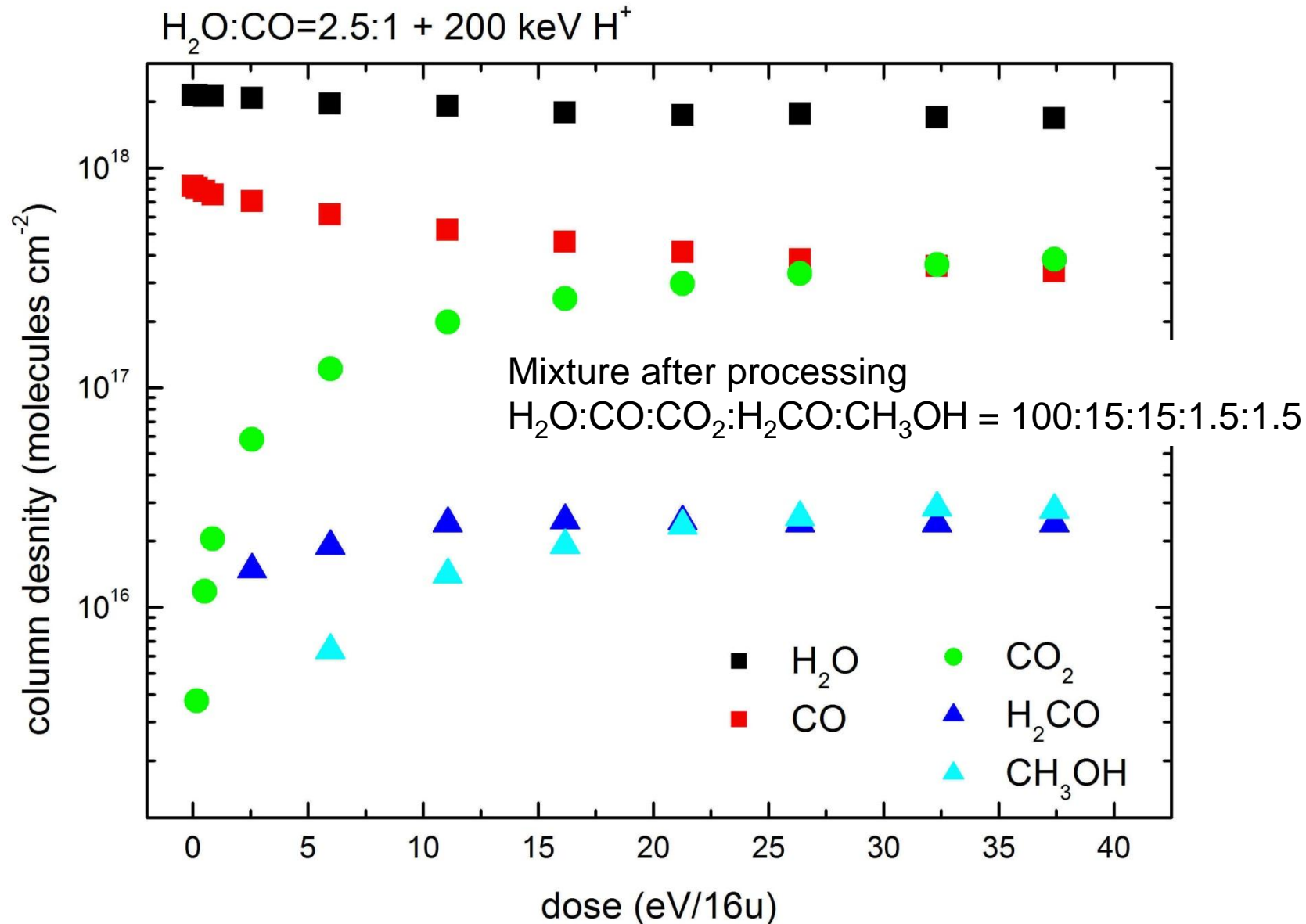


Laboratory experiments

$\text{H}_2\text{O}:\text{CO}$

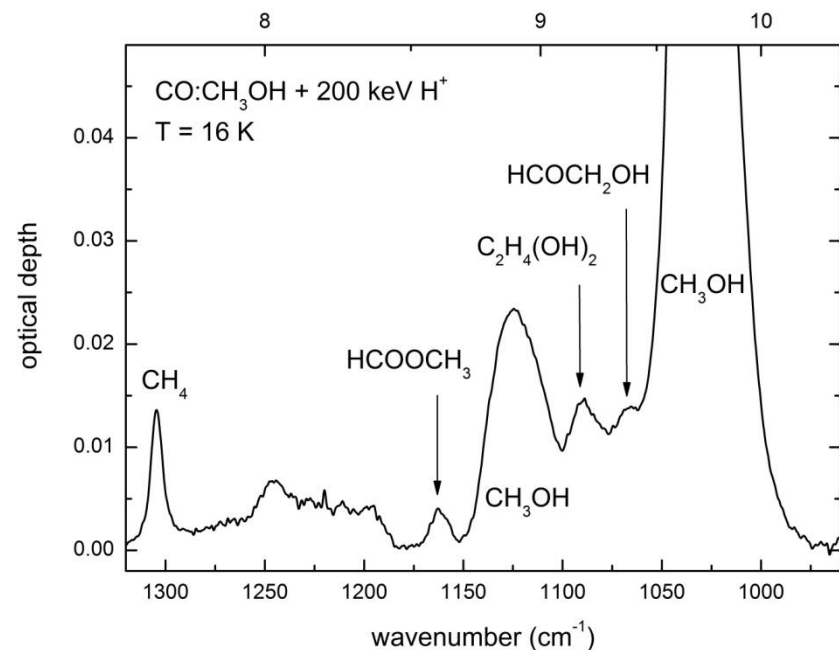
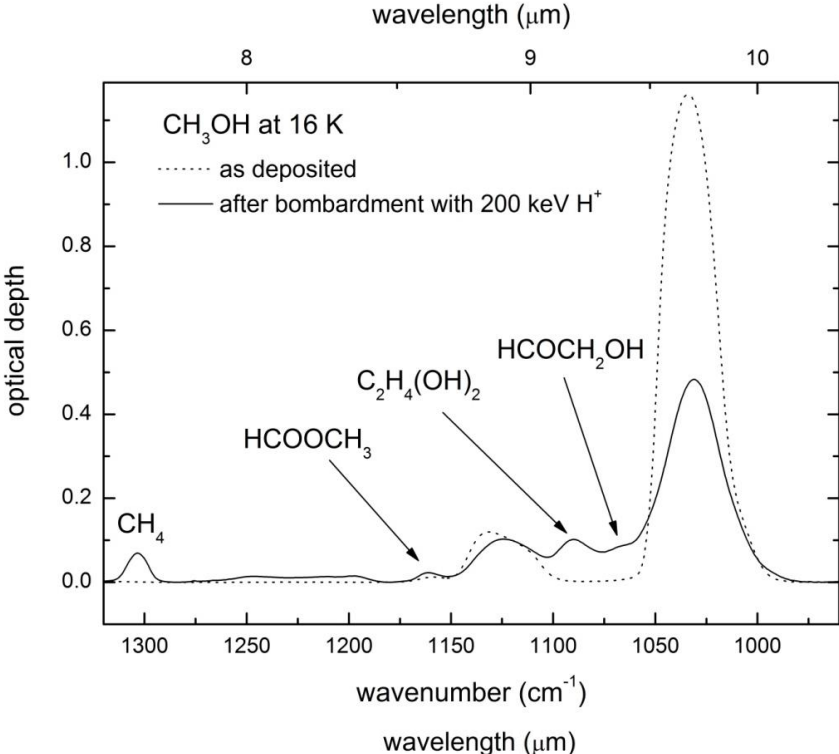
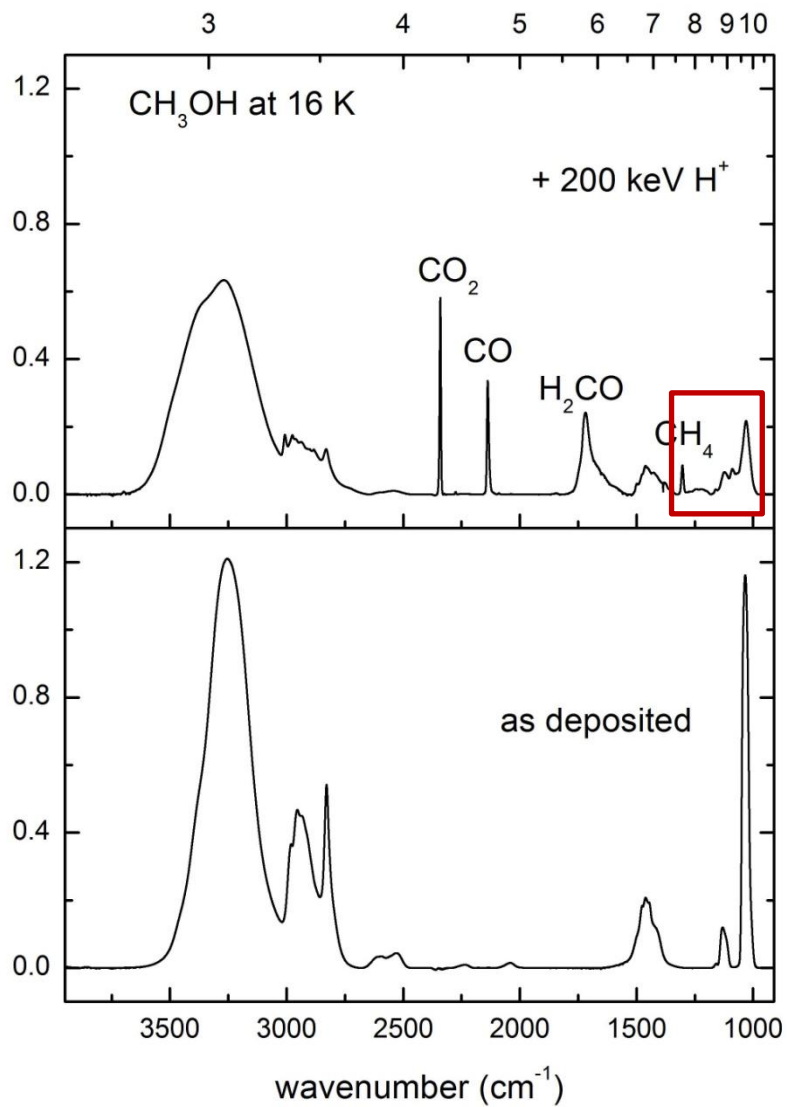


$\text{H}_2\text{O}:\text{CO}$

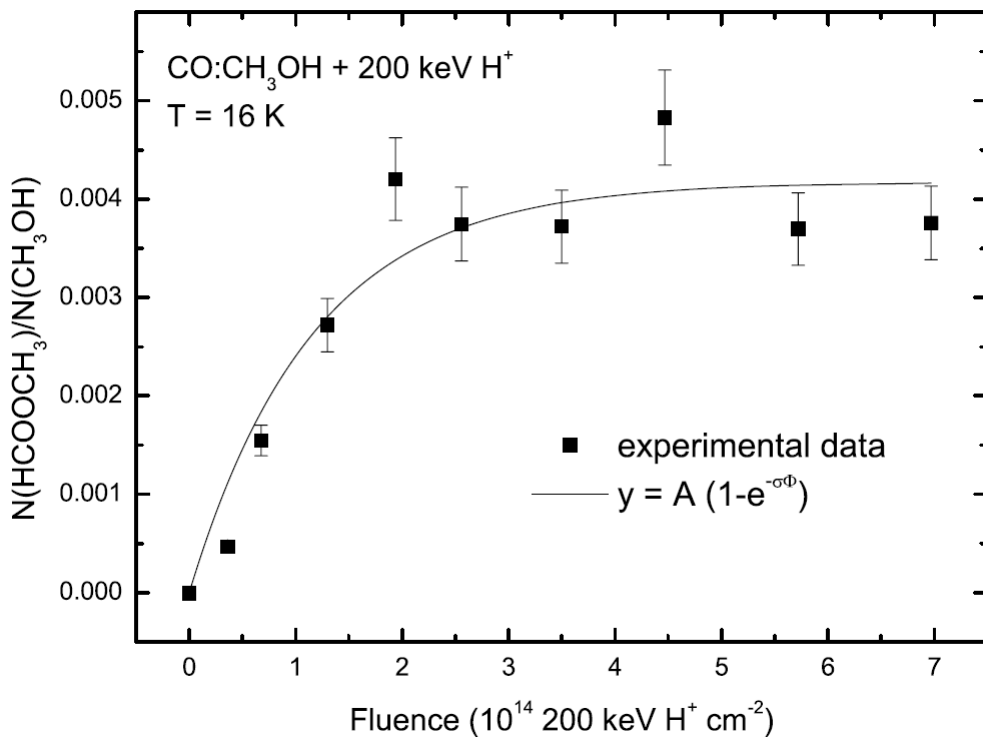


CH_3OH

optical depth



Formation rates



$$\zeta_0 = 3 \times 10^{-17} \text{ s}^{-1}$$

$$R(\zeta_0) = 6.2 \times 10^{-18} \text{ s}^{-1}$$

$$R(\zeta) = \frac{R(\zeta_0) \times \zeta}{\zeta_0}$$

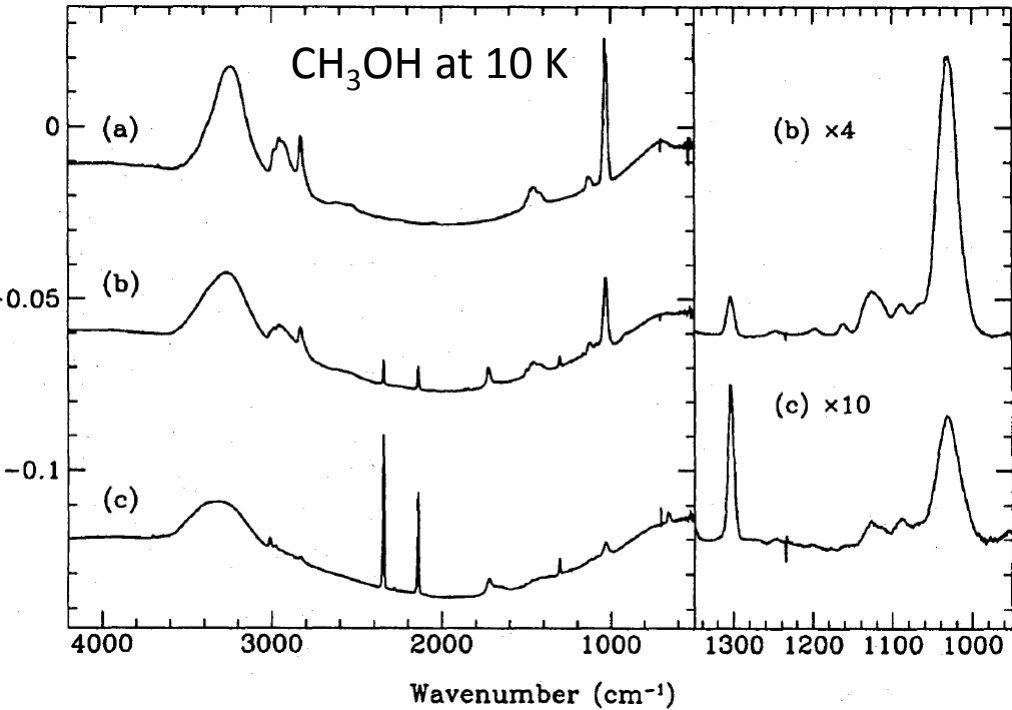
Occhiogrosso, A., Viti, S., Modica, P., Palumbo, M.E.
2011, MNRAS 418, 1923

Table 2. Observed and predicted column densities towards Orion KL hot core, G31.41+0.31, NGC 1333-IRAS2 and B1-b core.

Source	Type	Distance (pc)	T_{rot} (K)	Observations (cm ⁻²)	Model (cm ⁻²)
Orion KL Hot Core	High mass	480	250	$6.9 \times 10^{16} \text{ }^a$	3.5×10^{14}
G31.41+0.31 HMC	High mass	7900	300	$6.8 \times 10^{18} \text{ }^b$	9.3×10^{15}
NGC 1333-IRAS2	Low mass	220	38	$5.8 \times 10^{14} \text{ }^c$	6.4×10^{12}
B1-b	Dark core	350	<30	$8.3 \times 10^{12} \text{ }^d$	1.2×10^{12}

UV photolysis

ADSORBANCE



Gerakines et al. 1996, A&A 312, 289

Munoz Caro and Schutte 2003, A&A 412, 121

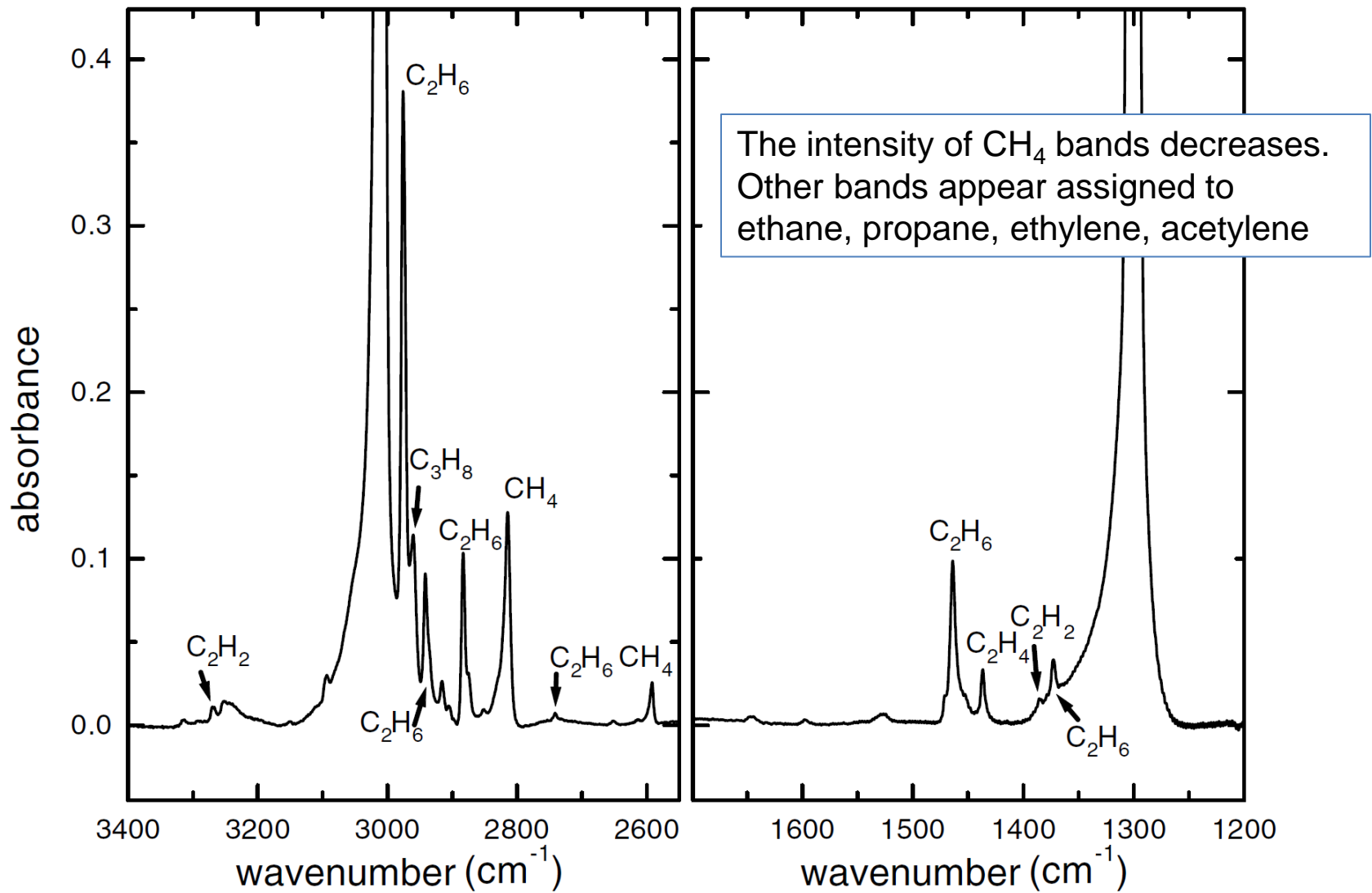
Oberg et al. 2009, A&A 504, 891

Islam et al. 2014, A&A 561, A73

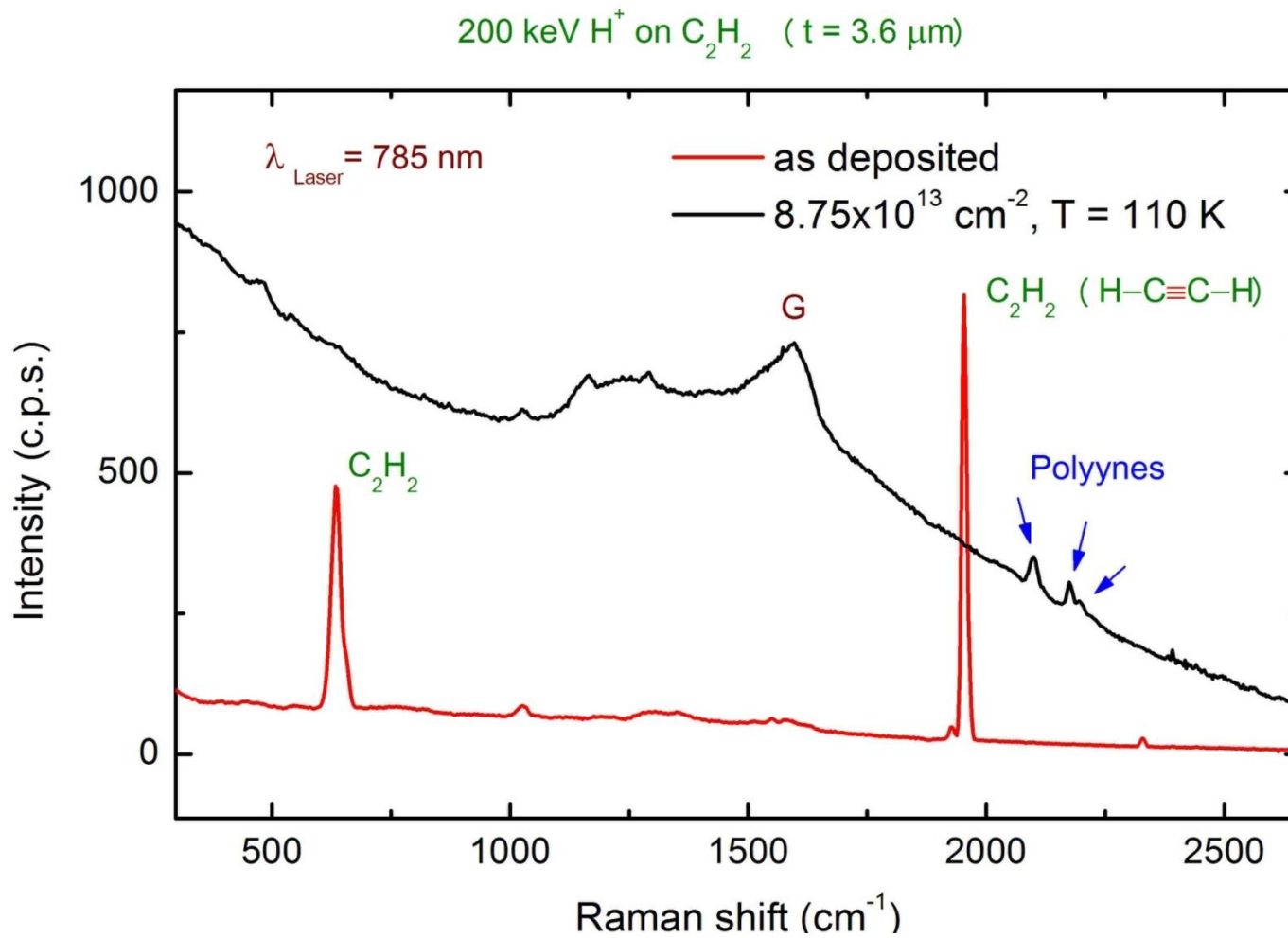
New bands observed during the photolysis of CH₃OH at 10 K

ν (cm ⁻¹)	Assignment
655	CO ₂
910	H ₃ COHCO
1088	C-OH stretch (alcohols)
1160	H ₃ COHCO; ν (C-O)
1197	CH ₂ OH
1244 ^a	H ₂ CO
1304 ^a	CH ₄
1352	CH ₂ OH
1497	H ₂ CO
1718 ^a	H ₃ COHCO
1719	H ₂ CO
1850 ^b	HCO
1863 ^b	HCO
2092	¹³ CO
2138 ^a	CO
2278	¹³ CO ₂
2342 ^a	CO ₂
3011	CH ₄
4140 ^a	H ₂

$\text{CH}_4 + 60 \text{ keV Ar}^{++}$ at 12 K



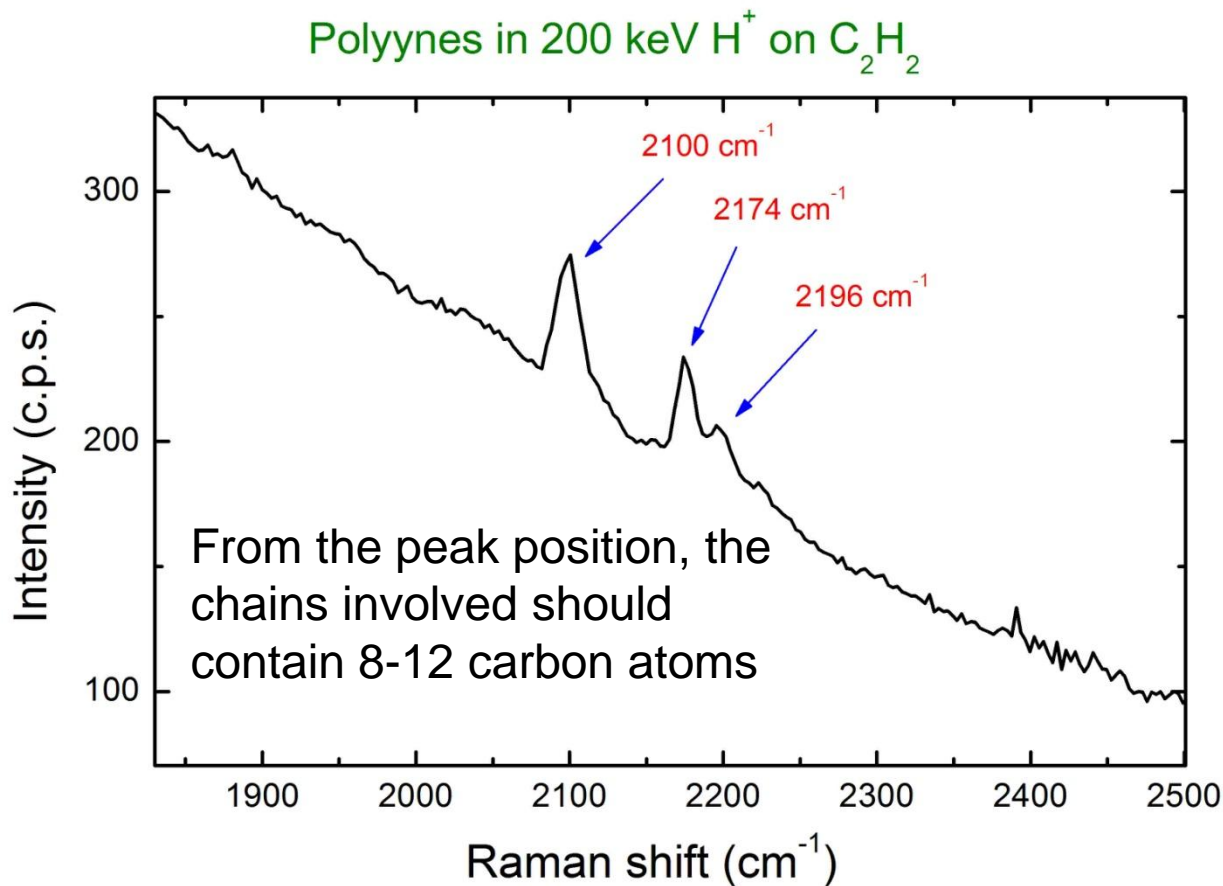
Formation of linear carbon chains



Compagnini et al. 2009, Carbon 47, 1605

Puglisi et al. 2014, NIMB 326, 2

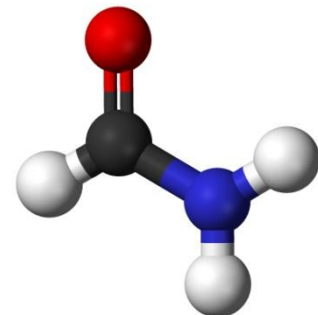
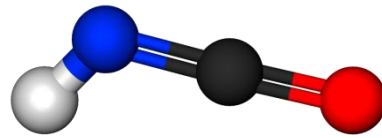
Formation of linear carbon chains



Compagnini et al. 2009, Carbon 47, 1605

Puglisi et al. 2014, NIMB 326, 2

Formation of formamide (NH_2CHO) and isocyanic acid (HNCO)



Studied mixtures

See poster presented
by Riccardo Urso

$\text{H}_2\text{O}:\text{CH}_4:\text{NH}_3 = 1:1:1 + 200 \text{ keV H}^+$

$\text{CH}_3\text{OH}:\text{N}_2 = 1:1 + 200 \text{ keV H}^+$

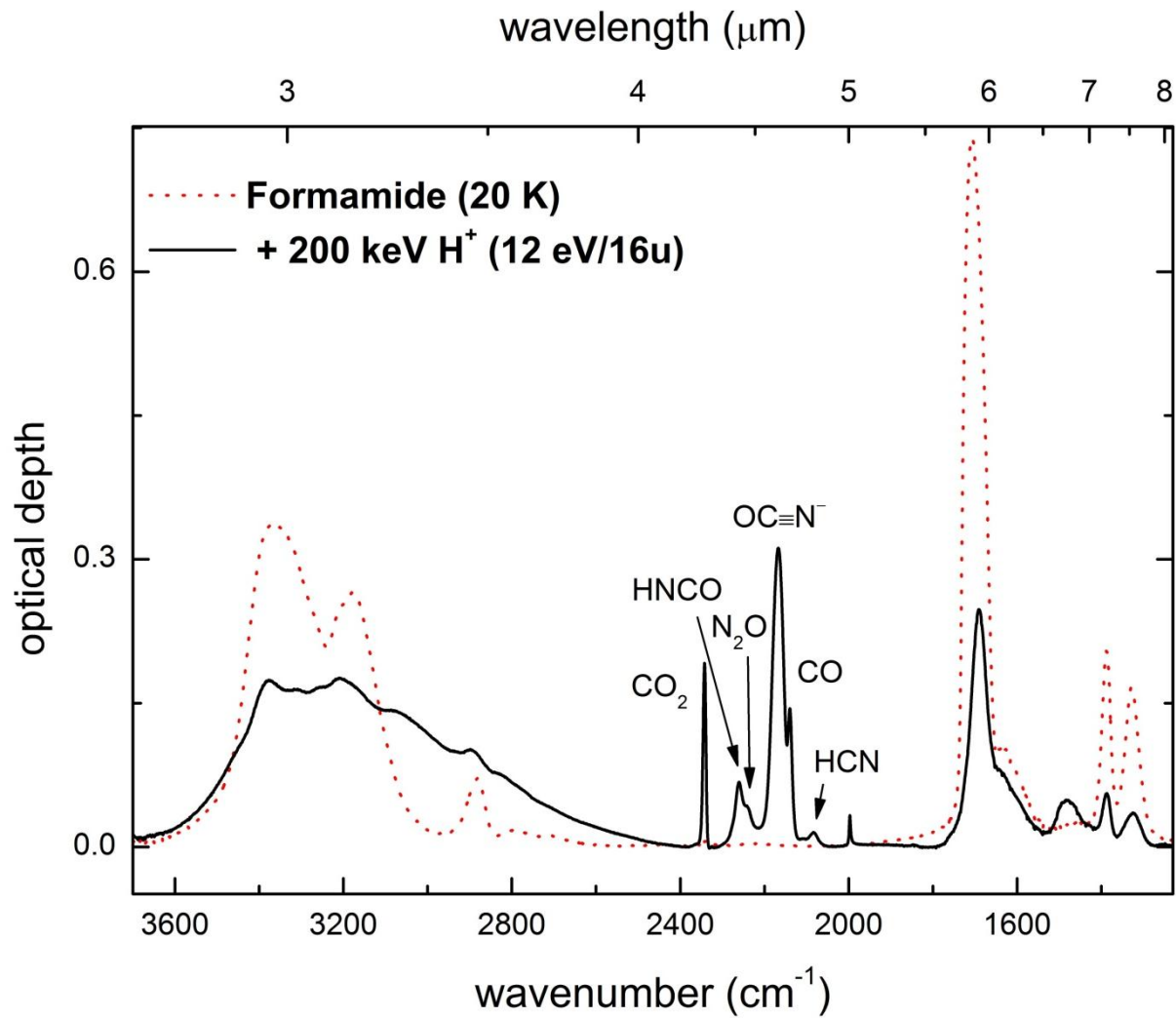
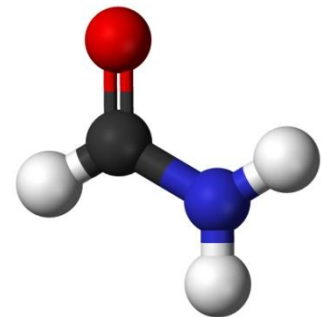
$\text{H}_2\text{O}:\text{CH}_4:\text{N}_2 = 1:1:1 + 30 \text{ keV He}^+$

$\text{H}_2\text{O}:\text{CH}_4:\text{N}_2 = 1:2:1 + 30 \text{ keV He}^+$

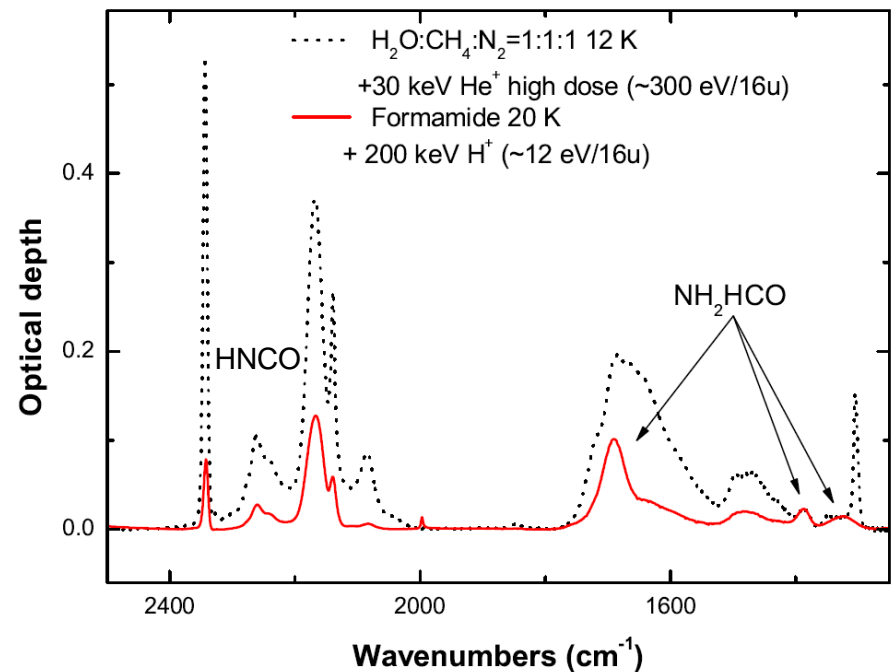
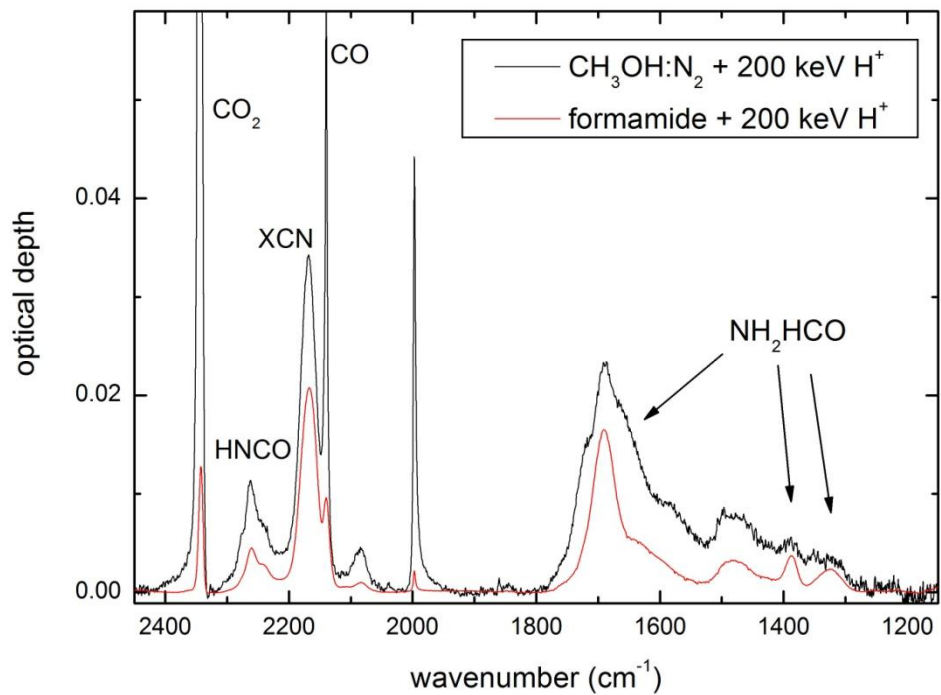
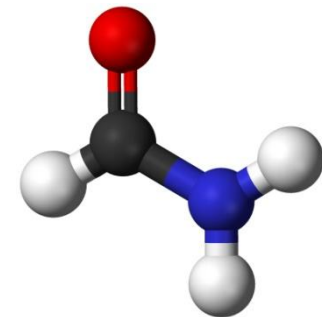
$\text{H}_2\text{O}:\text{CH}_4:\text{N}_2 = 1:2:10 + 30 \text{ keV He}^+$

$\text{H}_2\text{O}:\text{CH}_4:\text{N}_2 = 1:2:100 + 30 \text{ keV He}^+$

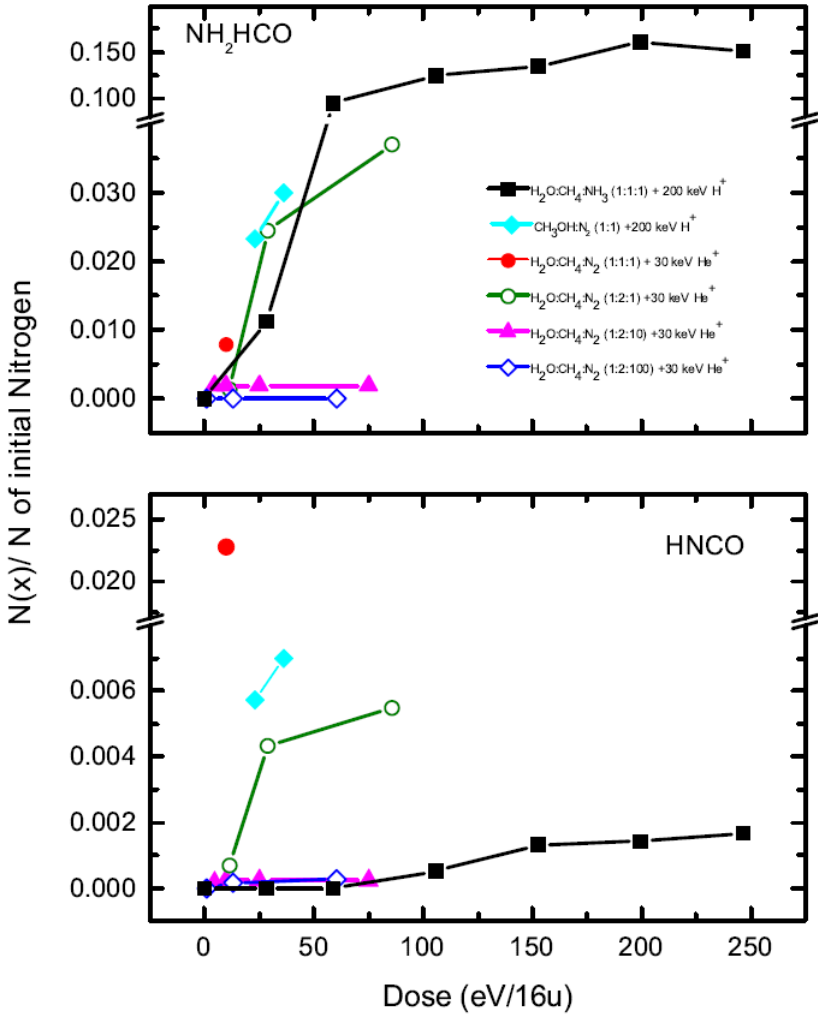
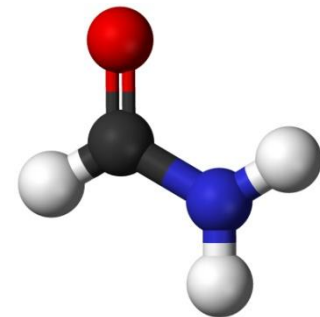
Formamide (NH_2CHO)



Formation of formamide (NH_2CHO) and isocyanic acid (HNCO)



Formation of formamide (NH_2CHO) and isocyanic acid (HNCO)



Experimental results

after dose = 10 eV/16u

$\text{NH}_2\text{CHO}/\text{nitrogen} \sim 10^{-2}$

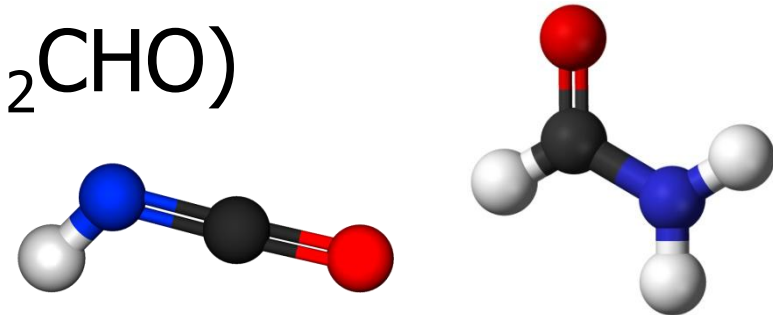
$\text{HNCO}/\text{nitrogen} \sim 10^{-3}$

Nitrogen cosmic abundance $\sim 2 \times 10^{-5}$

**Assuming high N-depletion
 NH_2CHO fractional abundance $\sim 10^{-7}$
comparable to observed values**

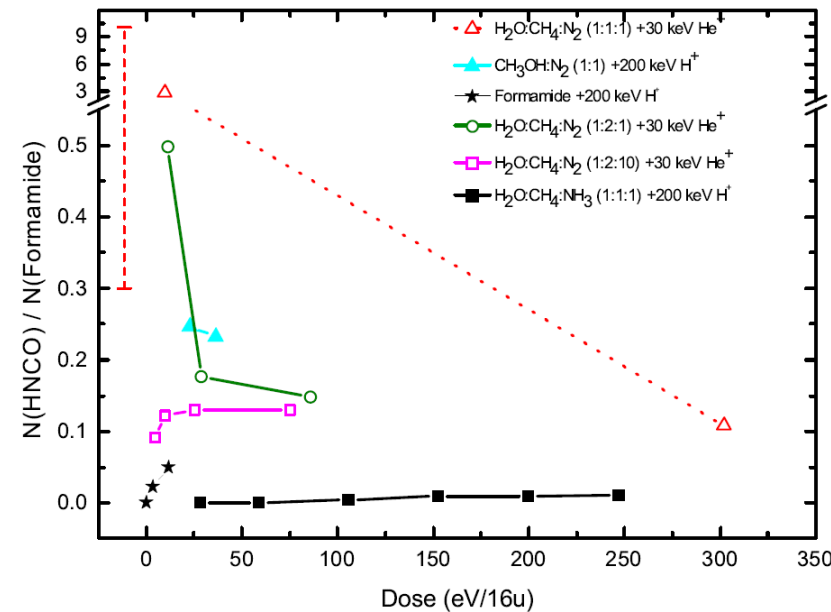
**HNCO fractional abundance $\sim 10^{-8}$
lower than observed values**

Formation of formamide (NH_2CHO) and isocyanic acid (HNCO)



dose (eV/16u)	timescale (years)			
	ionization rate (s^{-1})			
	1.3×10^{-17}	6×10^{-17}	3×10^{-16}	1.3×10^{-15}
1	1.1×10^7	2.5×10^6	5.0×10^5	1.1×10^5
10	1.1×10^8	2.5×10^7	5.0×10^6	1.1×10^6
100	1.1×10^9	2.5×10^8	5.0×10^7	1.1×10^7

While the observed amount of formamide can be accounted for by cosmic-ray bombardment of icy grain mantles, other processes (such as gas-phase and grain-surface reactions) have to be invoked to explain the observed gas-phase abundance of HNCO.



Formation of formamide (NH_2CHO)

A&A 576, A91 (2015)
DOI: [10.1051/0004-63](https://doi.org/10.1051/0004-63)
© ESO 2015

Result

The hydrogenation of HNCO does not produce detectable amounts of formamide

Hydrogenation at low temperatures does not always lead to saturation: the case of HNCO

J. A. Noble¹, P. Theule¹, E. Congiu², F. Dulieu², M. Bonnin², A. Bassas¹, F. Duvernay¹, G. Danger¹, and T. Chiavassa¹

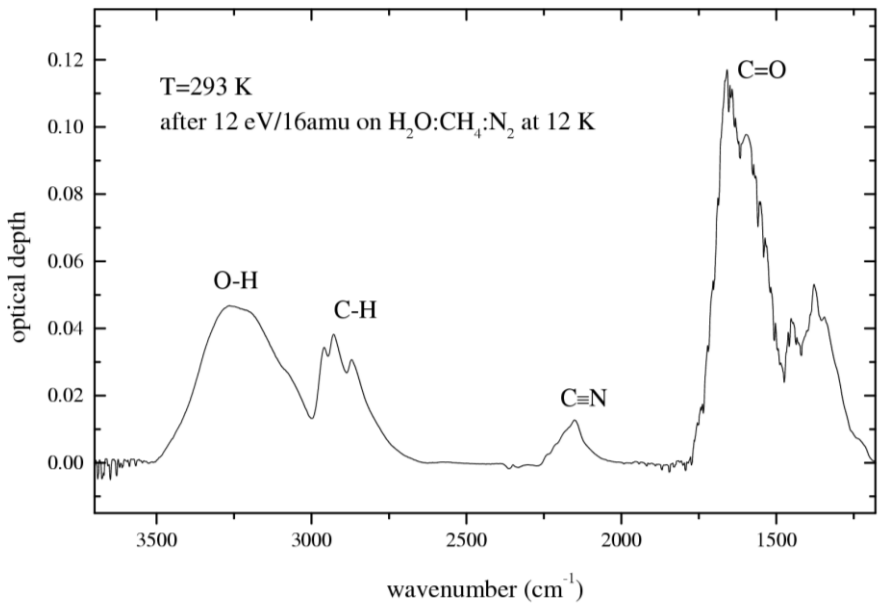
The major conclusion of this Letter is that there is no need to invoke grain-surface chemistry to explain the presence of formamide provided that its precursors, NH_2 and H_2CO , are available in the gas phase

Gas-phase formation of the prebiotic molecule formamide: insights from new quantum computations

V. Barone,^{1,★} C. Latouche,¹ D. Skouteris,^{1,★} F. Vazart,¹ N. Balucani,^{2,3,4}
C. Ceccarelli^{3,4,★} and B. Lefloch^{3,4}

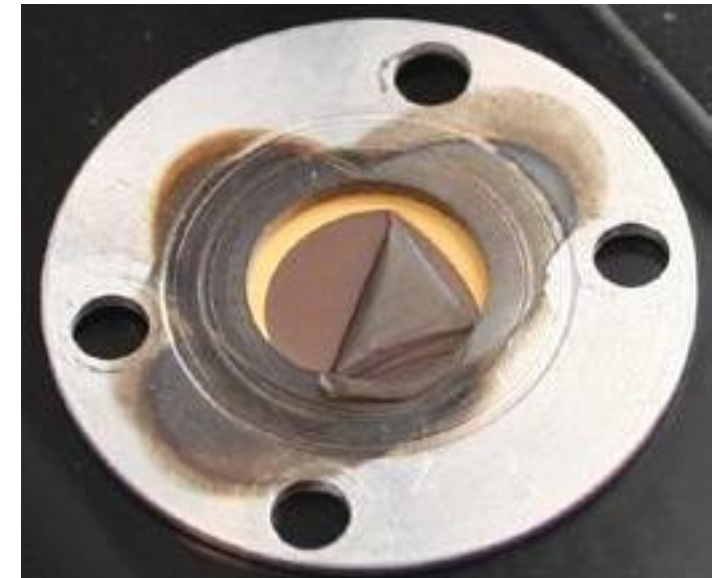
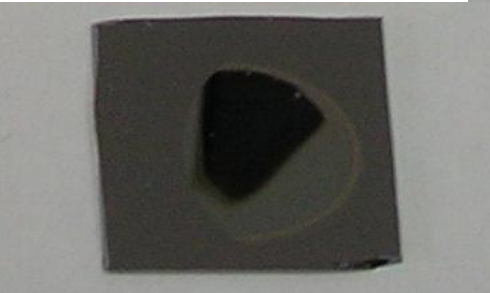
MNRAS 453, L31–L35 (2015)

Infrared and Raman spectroscopy of residues

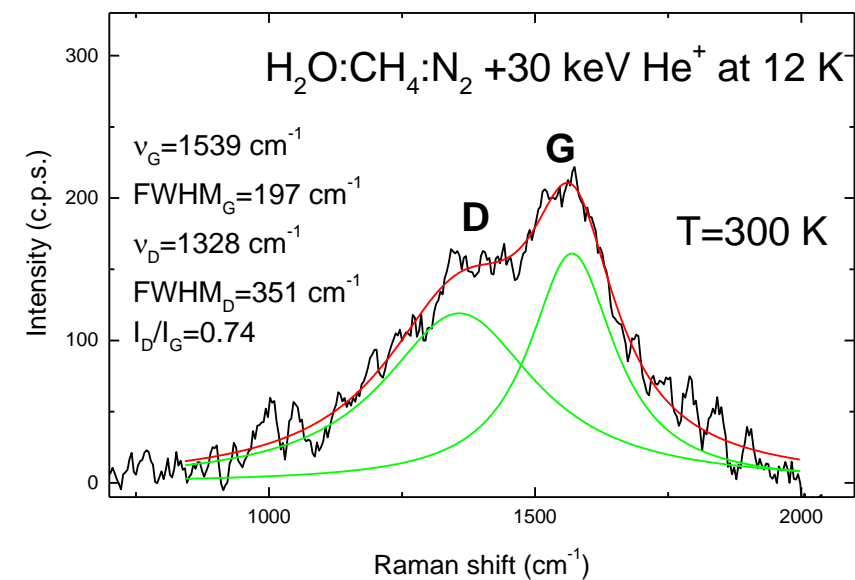
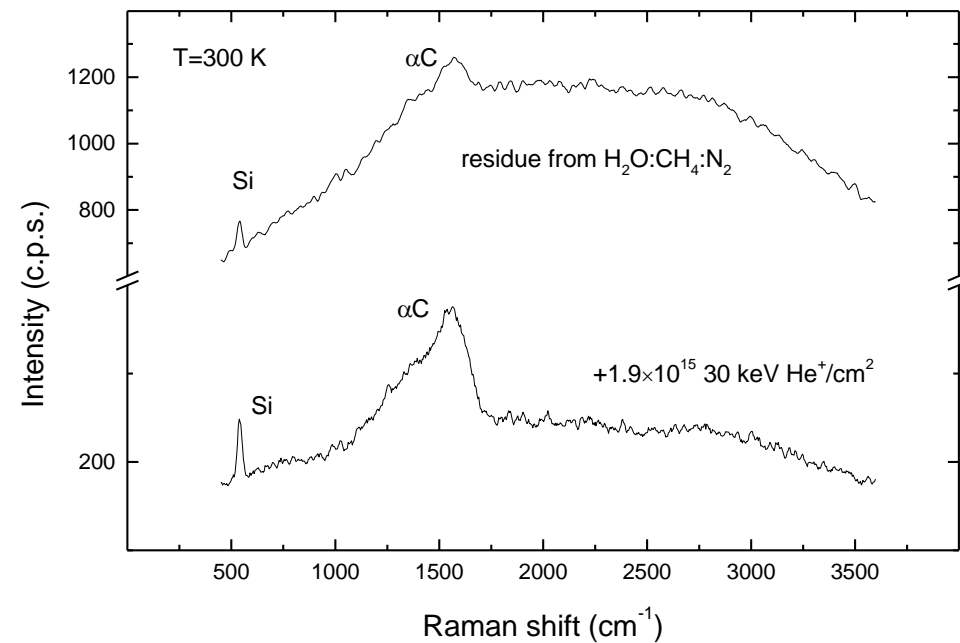


Strazzulla, Baratta, Palumbo 2001, Spectrochim. Acta A 57, 825
Palumbo, Ferini, Baratta, 2004, Ad Sp Res 33, 49

T=300 K

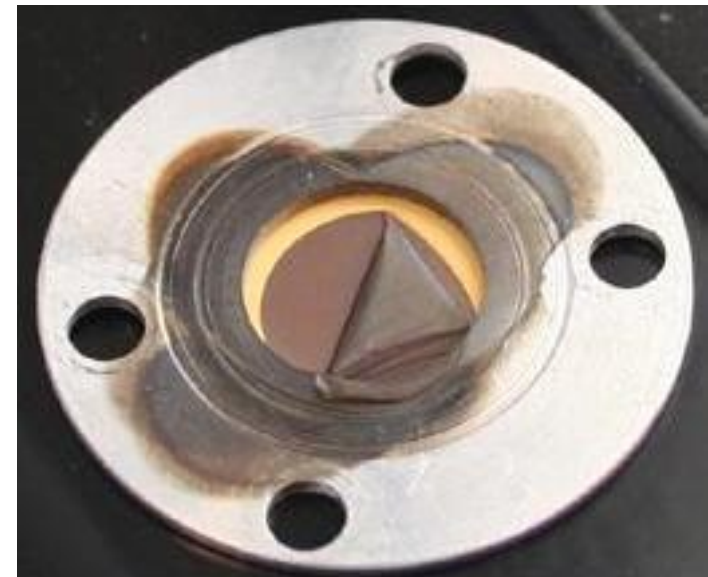
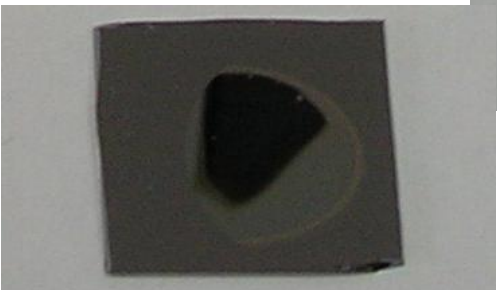


Infrared and Raman spectroscopy of residues

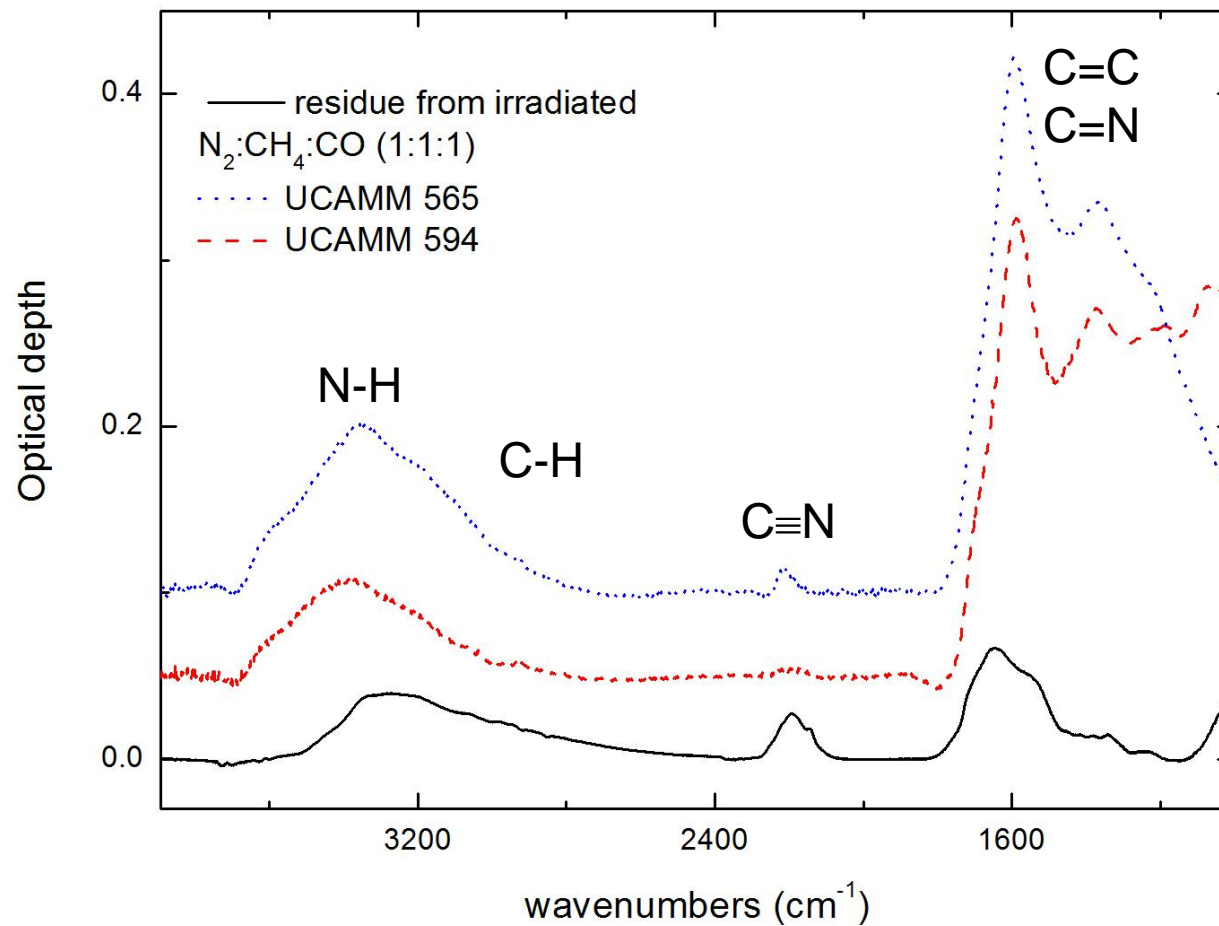


T=300 K

Ferini G., Baratta G.A., Palumbo M.E., 2004, A&A 414, 757



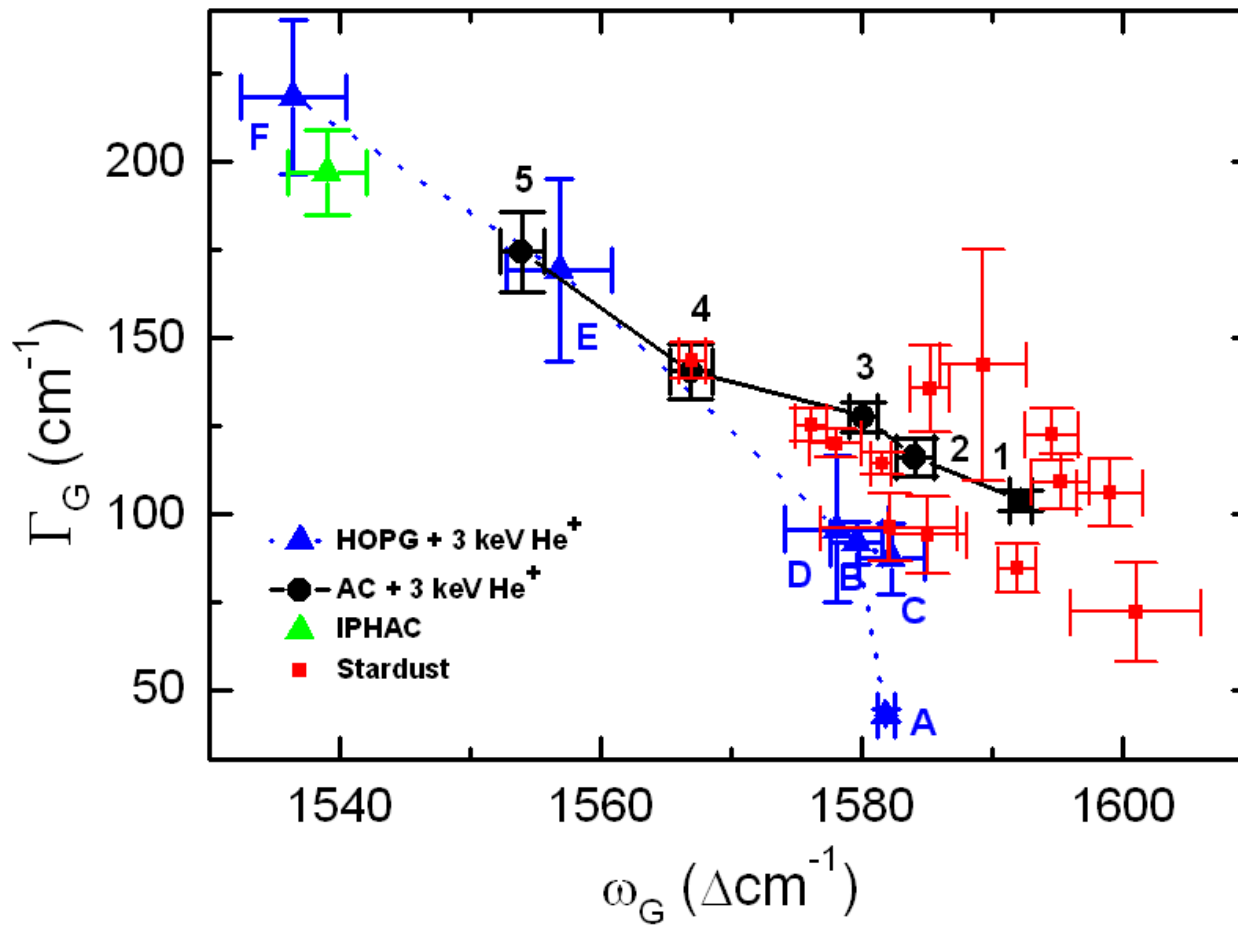
Ultra Carbonaceous Antarctic micrometeorites probing the Solar System beyond the nitrogen snow-line



Dartois et al. 2013, Icarus 224, 243

Baratta et al. 2015, Planet. Space Science, 118, 211

Comet Wild2 grains collected by Stardust

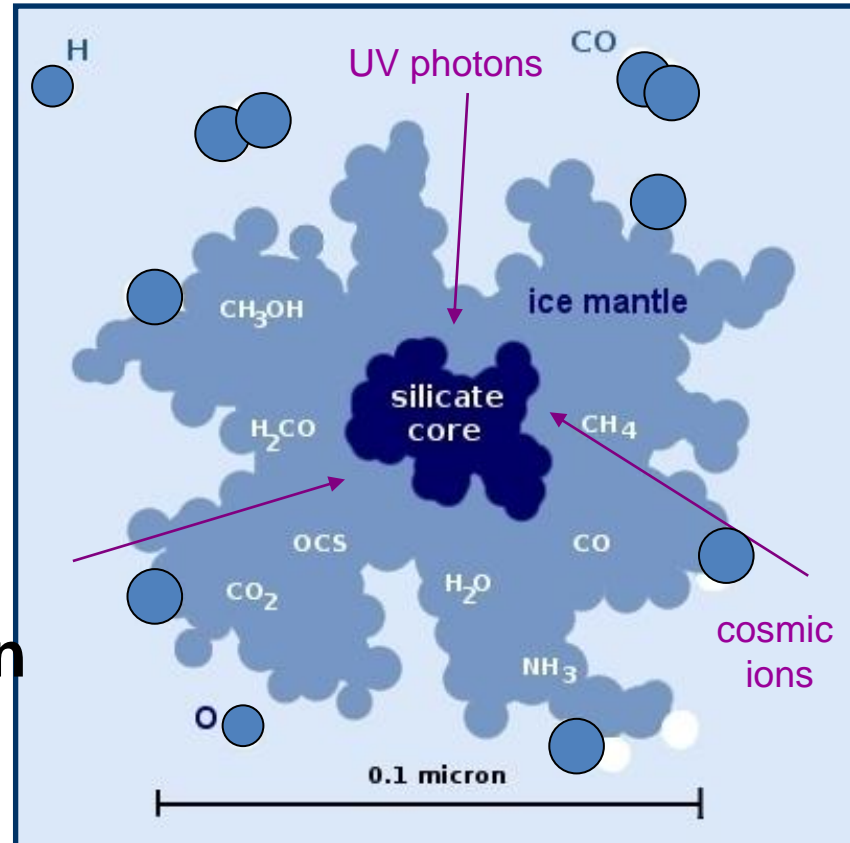


The most disordered amorphous carbon detected by Raman spectroscopy in some Stardust grains could be indicative of ion irradiation of carbon containing ices or of pre-existing more ordered carbons.

Summary

Energetic processing

- ✓ modifies the chemical composition of icy grain mantles;
- ✓ gives a significant contribution to the formation of complex molecules in the solid phase.



Molecules formed in the solid phase are released to the gas phase after desorption of ice mantles or are incorporated in planets, satellites and comets

Acknowledgments

Mario Accolla

Giuseppe Baratta

Giuseppe Compagnini

Saro Di Benedetto

Vincenzo Greco

Zuzana Kanuchova

Carlotta Scirè

Giovanni Strazzulla

Riccardo Urso



REGIONE SICILIA



INAF



Osservatorio Astrofisico
di Catania